

The UAV@LGL BW Project – A NMCA Case Study

MICHAEL CRAMER, Stuttgart

ABSTRACT

The flexible use of unmanned aircraft systems (UAS) in geodetic-photogrammetric applications has been demonstrated on several occasions, but mostly in the private sector environment. A proof of the suitability of this technology in the context of national mapping was not available so far – at least in Germany. Therefore, a pilot study of the Landesamt für Geoinformation und Landentwicklung Baden-Württemberg – the official mapping agency of Baden-Württemberg – and the Institute of Photogrammetry at University of Stuttgart was initiated to independently estimate the potential of UAS-based photogrammetric data acquisition. Two different camera systems were used in a land management application scenario. The georeferencing of the images was performed using Structure-from-Motion and photogrammetric bundle adjustment. Two different software lines are compared: The traditional Match-AT aerial triangulation is compared to the results from Pix4D. Similarly, two different approaches are also compared for creation of dense surface models. Here again the Pix4D is compared to the SURE dense matching software. The results of the study were able to meet all requirements of national mapping. From the national mapping's point of view a completely new method for the flexible and cost effective data capture is now available. New harmonized guidelines for the general flight permission will become available in medium term to simplify the formal-legal side of flight approval.

1. INTRODUCTION

Unmanned aircraft systems are now offering a variety of airborne platforms used in many different applications. When UAS is discussed in daily news today, typically military systems (often named drones) are in focus, which are used for pure military projects or dual purpose governmental applications. Following Blyenburgh (2013) about 2/3 of referenced UAS are in military or dual purpose applications. Less than 20% of systems are currently used for civilian commercial applications. The remaining are from research or in developmental scenarios.

About 50% of all the systems belong to the so-called micro and mini category. It is platforms with maximum take-off weight (MTOW) of <5kg (micro) or <25kg (mini) (Blyenburgh 2012). The MTOW in a way limits the flight endurance, the operational range, the maximum flight altitude and the available payload, which is the most important for the later application. It is this type of platforms, which quite often are used in civilian commercial applications including geodetic applications like mapping.

For sure, flight regulation also has to be considered. Up to now in almost all of the civilian operation scenarios flights are allowed within line-of-sight only. With that the area of interest should not exceed a circle of around 500 – 1000m radius, depending on the visibility of the UAS. The responsible pilot always has to guarantee to change from automatic flight to remotely controlled flight at any point of the mission. Larger areas have to be captured from multiple stations, i.e. the pilot will move to another position if the first part of the project is covered. Thus a large photogrammetric block will be formed from several smaller sub-blocks, each flown within the line-of-sight condition.

The use of UAS in geomatics was comprehensively demonstrated during the first UAV-g conference at ETH Zurich in 2011 (UAV-g 2011). It was shown that this type of sensor platform technology is mature and in principle can be used to acquire highly resolved airborne imagery. This imagery not only is used to provide orthomosaics and determine 3D object points but also dense point clouds for surface model generation can be derived.

With that UAS in principle became of interest for mapping agencies and might offer an alternative, maybe more flexible platform for airborne data acquisition. NMAs typically work on a national or

at least country wide level, where data are captured in regular update intervals. This type of data acquisition cannot be covered by current micro / mini-class UAS. Still, there are quite some scenarios even in national mapping, which are covering smaller areas only and where UAS can be used. Such governmental applications might be in

- cadastre, especially where direct access of land boundaries might not be possible;
- 3D mapping of any smaller area, for example for change detection. This might be changes in coast lines or cliffs, for example due to storm events, or changes in the Earth's surface for example in quarries or after infrastructure projects. Land consolidation projects also belong to this group of UAS scenarios. Here frequent flights for multiple data acquisitions might be necessary to document the project's progress to participants;
- emergency mapping, i.e. mapping of (local) flooding or after landslides in mountainous areas;
- monitoring, for example regular survey of flood protection devices like river or sea dykes.

In Cramer (2013b) the current status of UAS technology in the context of European national mapping agencies is presented. Quite interesting to see that all the NMAs considered for this report are well aware of UAS, some of them already have done their first empirical test flights, to become familiar with this type of data acquisition and to evaluate the performance of these systems. Some first experiences at IGN France and Ordnance Survey Britain are presented in Cramer (2013b). Here UAS is used for monitoring river Rhône dykes or rapid response orthophoto generation in urgent environments. van Persie (2013) is discussing the use of UAS in Dutch cadaster.

Within this paper the first UAS project officially conducted by the Landesamt für Geoinformation und Landentwicklung Baden-Württemberg (LGL BW), which is the survey authority of the state of Baden-Württemberg is presented. The project was designed as pilot test for all the 16 mapping agencies of the federal states of Germany, conducted in close cooperation with University of Stuttgart, Institute for Photogrammetry (ifp) in cooperation with the Institute of Flight Mechanics and Control (iFR).

The LGL BW, like all other national mapping agencies in Germany, is responsible for regular airborne image acquisition in defined update cycles. The whole state of Baden-Württemberg is covered with images of GSD 20cm every three years, mainly for orthophoto production. Special needs – currently there is a project to split fees for waste water discharge calculations – require additional flights with even higher resolved images. Here images with 10cm GSD are flown, again covering almost the entire state of Baden-Württemberg, but mainly focusing on the built up areas. It is quite clear, that these two requirements cannot be solved with UAS technology. In addition LGL BW is also involved in land consolidation and land management projects. It is interesting to see, that there are currently (as of Spring 2013) almost 500 different land consolidation projects in the state of Baden-Württemberg, which cover approximately 10% of the size of the country! All these projects cause a high number of additional photo flights; usually GSD values <10cm are required which are not part of the standard flight missions. As these consolidation projects run over several years, the progress of the project has to be documented. Images and continuously updated orthophotos provide very helpful data to also inform and involve land owners in this land consolidation procedure. Thus multiple flights are necessary for each of these projects. As the area per project is typically quite small, financing these extra flights is always of issue. This is the frame where UAS technology may come into operational use in case the UAS derived products will fulfill the required specifications. Thus the empirical test presented in the following sections was designed as part of a land consolidation project of LGL BW.

2. TEST FLIGHTS

2.1. Test site Hessigheim

The empirical UAS flights were flown in an area nearby the small village of Hessigheim in the Neckar river valley, around 25km north of Stuttgart, Germany. The area which, was selected by LGL BW for the UAS data acquisition is the so-called Hessigheimer Felsengärten: a steep vineyard, with rocks and vegetation. The area of interest has an extension of 1000m x 400m with height differences of about 100m on a 200m distance only (Figure 1). From photogrammetric point of view this is a quite demanding area because of steepness and land cover. From UAS point of view, it is quite favorable as the UAS is visible during the whole flight as long the remote pilot is approximately centered in the middle of the area. Thus the area can be flown in one block without violating the line-of-sight condition. In Figure 1 the location of check and control points are also indicated; Figure 2 depicts their positions in a more detailed view. For the later accuracy assessment the highlighted points (red triangles) are used as check points. It is altogether 33 points in object space in the area of interest, all signalized prior to the flight campaigns through LGL BW. Their coordinates were measured with static GPS. The standard deviation of these object point coordinates (accuracy) is within 1-2cm.

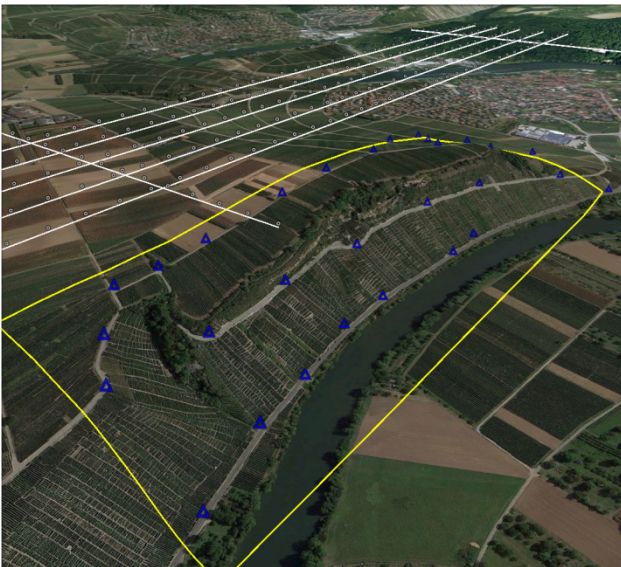


Figure 1: Hessigheim test site for UAS flight campaign, with UAS flight lines.



Figure 2: Hessigheim ground control and check point configuration (as used in later processing). Check points are highlighted in red.

2.2. UAS sensor platform

As it was already discussed in Section 1. , it is UAS of mini or micro category which are used for mapping in civilian applications often. This to a certain extent is due to the limitations for flight permission, which are not discussed in detail here. Some more details can be found in (Cramer et al. 2013c). In short, to get approval to fly an UAS is getting more difficult, when the overall weight of the system (MTOW) increases. In many countries 5kg is such threshold, which affects the complexity to get permission to fly; this is why many UAS are below 5kg MTOW.

The Institute of Flight Mechanics and Control (iFR) at University of Stuttgart has access to different UAS platforms. As the Hessigheim test from its site extensions is still close to a standard photogrammetric project (elongated rectangular mission area), and the site is relatively big from

UAS point of view, the flights were done with a fixed-wing UAS. Rotary-wing UAS are more flexible especially when more locally areas, i.e. single buildings are of interest. The flights were done with two different carriers, both below 5kg MTOW (UAS category micro) – the Multiplex Twinstar II and the Bormatec Maja. A second carrier became necessary as the imaging sensor was changed during the project which requested for a higher payload capacity. The Maja Bormatec is a commercially available platform, already prepared for the recording of aerial photography (Bormatec 2013). The hull can be opened to almost full-length. The single-engine aircraft (propeller at the rear behind the tail) is made of expanded polypropylene (EPP), like the Twinstar II, and is also landed on the hull. More details on the carrier and the onboard electronics can be seen from (Cramer et al. 2013c).

Standard off-the-shelf 12 Mpix consumer grade cameras were used for imaging. The Canon Ixus 100 IS was used for the first flight campaign; later this camera was exchanged by a Ricoh GXR Mount A12 system camera in combination with a Carl Zeiss Biogon lens. Some of the basic camera parameters can be seen in Figure 3. The Canon came into market in 2009 already, the Ricoh/Zeiss was ordered in May 2012.

In order to evaluate the performance of both systems, several investigations on geometric resolution were done. The tests were made by using a Siemens star pattern, imaged in terrestrial environments as well as during airborne over flights. In Figure 4 two examples are shown, where the left shows the Siemens star (8 m diameter) from the Canon, the right from the Ricoh/Zeiss flight. The images were taken during the flight, the distances between camera and target were slightly different but around 175m, which corresponds to a nominal GSD of around 4.5 and 5.0 cm. The results obtained from analysis of point spread functions derived from the Siemens star is given below the figure. Different quality measures, referring to image and object space are given. As one can see, the empirical resolution of the Ricoh/Zeiss imagery is always better than the Canon, which also indicates the higher radiometric performance of the Ricoh/Zeiss system. More details on the camera performance testing and the later geometric calibration can be seen in (Cramer et al. 2013a).

	Canon Ixus 100 IS	Ricoh GXR Mount A12 & Zeiss Biogon 21mm
No. of pixel	4000 x 3000	4288 x 2848
Pixel size	1.54 mm	5.5 mm
Sensor size	6.16 x 4.62 mm ²	23.6 x 15.7 mm ² (APS-C format)
Lens	Zoom, 5,9 (W) – 17,9 (T) mm	Fixed focal lens, 21 mm
Weight	180 g	650 g



Figure 3: Cameras used for the UAS imaging.

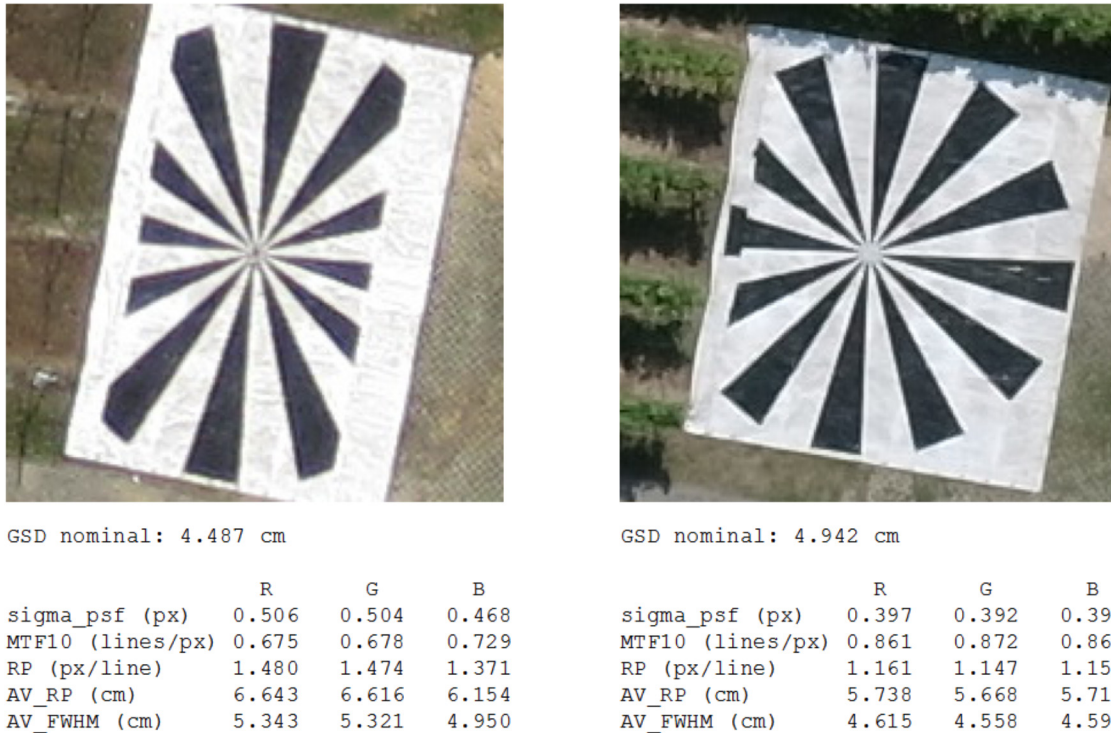


Figure 4: Geometric resolution of Canon Ixus (left) and Ricoh/Zeiss (right) cameras.

2.3. Image data acquisition

The flight was designed based on the expectations from LGL BW. LGL BW asked for oriented airborne imagery with $GSD < 10\text{cm}$ and an orthophotomosaic of same GSD. The flights were planned with a nominal ground pixel size (GSD) of $4.5\text{cm} - 7.3\text{cm}$. The variation of the GSD is due to the terrain height differences, as already mentioned before. Large overlaps within flight and across flight directions have been chosen in order to have optimal coverage for the later generation of dense point clouds. Higher overlaps additionally absorb for the much higher tilt and roll angles for the UAS flight, which also influence the resulting overlap between neighboring images on ground. Finally a total of 5 strips and two cross strips with approximately 80% overlap within the strip and $>70\%$ between adjacent strips were defined, as already shown in Figure 1. Altogether two flight campaigns have been flown, the first flight was done in March 2012 using the Twinstar II / Canon UAS setup, the second flight was done in August 2012, where the Maja / Ricoh/Zeiss system installation was flown. As both cameras have very similar camera geometry, the flight parameters remained unchanged for both flight campaigns.

3. DATA PROCESSING

The data processing is divided in the image georeferencing part and the generation of photogrammetric products, where main focus is on the generation of dense 3D surface models. For both steps, two independent process lines are available: The UAS process chain which is established at ifp is based on the Trimble/inpho Match-AT for the image orientation and additional own software components for image pre-orientation and dense surface model generation. This is compared to the commercial software Pix4D, which is especially designed for processing of UAS image blocks and covers the whole processing chain in one single software environment.

3.1. Image Georeferencing

The first major step in processing of photogrammetric imagery is the georeferencing of the data. This typically is solved within an aerial triangulation, where overlapping images are connected via tie points. With the support of ground control points (and optional directly measured exterior orientation elements, if available) the data is finally transformed to the object coordinate frame. The ifp has established a slightly modified processing chain for the UAS data, where the large(r) deviations of UAS imagery from traditional normal case geometry are taken into account. The processing of imagery starts with a Structure-from-Motion (SfM) method, which originally is from the computer vision. SfM allows for the orientation of in principle arbitrarily arranged image blocks. The connection of images is done via SIFT points. An example of such SfM approach is the Bundler software developed within the Photo Tourism project (Snavely et al. 2008). The SfM used in the ifp processing chain is described in Abdel-Wahab et al. (2012 & 2011). It is based on a modified approach of Farenzena et al. (2009). After SfM has applied, the block is formed (i.e. images are tied together via SIFT feature points). Exterior orientations are available in a local coordinate frame as no external control information has been involved so far. Thus the GPS perspective centre coordinates are used to transform the whole image block into the final object coordinate frame. With that each image has its exterior orientation, which then can be used as initial values to set-up the aerial triangulation project using standard photogrammetric software like Trimble / inpho Match-AT.

A more straight-forward UAS image processing would be realized, if the SfM (i.e. the georeferencing of arbitrarily oriented image blocks) is already solved in the final object coordinate frame. As an example the Pix4D software is introduced, which always considers the GPS perspective centre coordinate observations during the processing to directly transfer the block into the final 3D object frame. Additionally control points can also be involved. With that the full georeferencing of UAS blocks can be solved within one software, there is no need to export the SfM results into any other photogrammetric software package. The Pix4D processing is based on the SfM approach and not only solves for the image georeferencing, but implements the full photogrammetric processing chain from the georeferencing to surface model generation and orthophoto mosaicking in just one step (Küng et al., 2011).

3.2. 3D point cloud generation

Image based 3D point cloud generation changed tremendously with the availability of dense matching software. It was all initiated by the so-called semi-global matching (SGM) proposed by Hirschmüller (2008). The SGM performs a stereo matching for each single pixel and thus produces very dense point clouds. In addition, the strong overlaps between imagery allow for a combined pixel wise matching of multiple overlapping stereo models. Thus, multiple redundant stereo measurements are available per pixel, enabling a significant increase of accuracy, completeness and reliability of the derived 3D point cloud (Haala 2011). For processing of dense point clouds the SURE dense matching software was used, developed at ifp (Rothermel et al. 2012).

Because of the large overlap between images, multiple stereo partners are available for each pixel in the base image. With that a highly redundant determination of the corresponding 3D point is possible. Errors in parallaxes and noise in the generated 3D point clouds is reduced. Finally, a 3D object point is generated only when it is consistently determined from at least two stereo models. Digital Surface Models (DSM) are then derived from the very dense 3D point clouds. The mean GSD of flights of 6cm defined the grid size of the resulting grid. Usually, several 3D points from the dense stereo matching are available for each grid cell. In order to ensure sufficient reliability of the grid cells, no height value is assigned with less than three points. For all other cells both height and the color value are determined by calculating the median of all 3D points within each cell.

As already mentioned in the previous sub-section, the Pix4D also generates dense surface models. Unfortunately there is no detailed information on the implemented surface model generation. As described in Strecha et al. (2012) a first 3D surface model (irregular triangulated net) is obtained from triangulation of adjusted 3D object points from image orientation process. As mentioned there, “At this stage, construction of a dense 3D model [...] increases the spatial resolution of the triangle structure.” No further details can be made on the internal processing of dense surfaces in Pix4D.

4. EMPIRICAL RESULTS

4.1. Image Georeferencing

Within this part the georeferencing of the empirical UAS imagery is discussed. As already mentioned, two flights had been done, using two different UAS carriers and two different cameras. The Canon block, was flown on March 23, 2013 with 202 images, the Ricoh/Zeiss images were taken on August 23, 2013. 190 images formed this block, the block layout can also be seen from Figure 2. The aerial triangulation was done using the Match-AT software (Applications Master version 5.4.1), where the results from SfM pre-processing were introduced as starting values. Only standard AT based on control points was considered, no additional GPS perspective centre coordinates had been involved. The quality (RMS) of 3D object point determination is derived from check point differences. The same 11 check points are used for all different AT runs. The configuration of control and check points was depicted in Figure 2 already. Additionally, the precision of 3D points from error propagation described the theoretical accuracy (precision). In order to compare results from Match-AT to Pix4D (version 2.2.3 (build 2.2.11) used), the same manual image observations have been used, i.e. the image coordinates of control and check points had been measured in Match-AT and then imported to Pix4D. All control points were introduced with the same weights (Std.Dev. 2cm) for both Pix4D and Match-AT processing. Table 1 shows results for the two flights using different observations (i.e. different tie point measurements) and software.

	sigma0 [pix]	Std.Dev [m]			RMS [m]		
		East	North	Up	East	North	Up
Canon – Match-AT							
tie pts: SIFT (SfM)	0.7	0.036	0.032	0.141	0.050	0.037	0.095
tie pts: Match-AT (LSM)	0.3	0.008	0.007	0.024	0.030	0.023	0.050
Ricoh/Zeiss – Match-AT							
tie pts: SIFT (SfM)	0.7	0.034	0.030	0.110	0.031	0.037	0.058
tie pts: Match-AT (LSM)	0.3	0.018	0.015	0.049	0.029	0.024	0.043
Ricoh/Zeiss – Pix4D							
	n.a.	n.a.	n.a.	n.a.	0.017	0.014	0.061

Table 1: Quality of georeferencing using Match-AT and Pix4D. 22 ground control points are used in processing. The RMS values are derived from 11 check points. The Std.Dev. of 3D object points is estimated from error propagation. Std.Dev. and sigma0 are not available from Pix4D.

For Match-AT processing, two different tie point configurations have been used. In a first run the tie points obtained from SfM have been imported to Match-AT directly, those points are derived from SIFT features. Second, the tie points have been re-measured using the Match-AT automatic tie point matching. This is realized through image pyramids using traditional feature based matching (FBM) to get first approximations followed by least squares matching (LSM) to increase matching quality. From theory the LSM should offer point matching accuracy up to 1/10 pix, which is

significantly higher compared to the feature based methods. This can be seen in the estimated qualities, comparing the results based on SIFT feature points, to the results, when tie points from Match-AT LSM are used for image observations. In both cases there is a significant increase in Std.Dev. and RMS values. The σ_0 is increased from 0.7pix to 0.3pix, which is mainly due to the higher quality of LSM matching compared to SIFT feature points. In principle, it also is possible to refine SIFT points by subsequent gray value-based matching as shown by Remodino (2006). But this was not applied for the SIFT points used for later Match-AT.

In the Match-AT processing no additional self-calibration was considered, as the images already had been pre-corrected by the interior orientation including lens distortions. Shortly before flights, each camera had been geometrically calibrated via test-field calibration. Then each image from flight mission has been resampled applying these interior orientations to derive almost distortion free images before images have been used in AT. In Cramer et al. (2013c), the influence of additional self-calibration in Match-AT is investigated. Self-calibration hardly has any influence for these pre-corrected images, which also shows, that both cameras are quite stable during flight.

Only the Ricoh/Zeiss flight was processed in Pix4D, as explained in Section 3.1. The Pix4D matching is based on a modified version of the SIFT feature matching. An improved version of the binary descriptors proposed in Strecha et al. (2012) is used. Different to Match-AT, Pix4D always refines the camera parameters. Obviously a physical camera model, as originally proposed by Brown is implemented. For the Ricoh/Zeiss image block the principal point and focal length was improved by a factor of around 0.2%, which is very small. The coefficients for radial and tangential are almost negligible and less than 0.001. This again shows that pre-correction of images worked quite well. Still, even such small corrections will influence the later results.

The Pix4D does not provide a thorough statistical analysis of results, but a mean re-projection error and the absolute accuracy (RMS from check point differences) are given in the report file. As the same 11 check points have been used always, the RMS values from Pix4D processing directly can be compared to the accuracy obtained from Match-AT. The mean re-projection error is 0.17pix which is of the same accuracy than the Match-AT results based on LSM tie points. Even though the definition of re-projection error is not exactly the same as σ_0 the comparison shows the high quality of point matching in Pix4D, which is due to the improved key point matching. Especially the difference to Match-AT based on SIFT points is visible. In addition, the slightly refined camera calibration also may have positively influenced the results. Comparing the RMS values, Pix4D obtains slightly better results in horizontal components. The vertical accuracy is slightly worse compared to the Match-AT run using LSM point matching. Still, the overall quality of Pix4D compared to Match-AT (LSM tie points) is fully comparable.

4.2. Surface model generation

The surface model generations relies on the results from image georeferencing. Only the results from Ricoh/Zeiss block are considered here, details on the DSM derived from the Canon image block and the comparison between Canon and Ricoh/Zeiss DSM can again be found in Cramer et al. (2013a, 2013c). Two DSMs were generated: the SURE DSM relied on the exterior orientations from Match-AT (LSM) processing; the DSM derived from Pix4D is based on the Pix4D orientation. Performance of image georeferencing was shown in Table 1. As the quality of georeferencing is very close, the two different exterior orientations should not affect the DSM generation too much. Thus, the two DSMs can be compared. The final DSMs, i.e. the filtered and interpolated point clouds, are of similar raster width referring to the mean GSD. It is 6cm for the DSM from SURE, and was automatically defined to 6.1cm for the Pix4D DSM.

The Pix4D DSM was processed with its standard parameter settings: Optimal 3D point density, medium surface smoothing type and optimal surface smoothing radius (16 units). Further runs with

slightly modified settings did not improve the Pix4D DSM, thus only this DSM is discussed here. The SURE assumptions for processing already were mentioned in Section 3.2.

Figure 5 shows the colored surface model for the whole area. This result is obtained from SURE. The area is completely modeled, except the very steep parts and some of the vegetation areas, as it would be expected for airborne non-oblique imagery. A more detailed zoom-in is given in Figure 6, for the small highlighted area in Figure 5.



Figure 5: Surface model test site Hessigheim (SURE). The highlighted part will be illustrated in more detail in Figure 6.

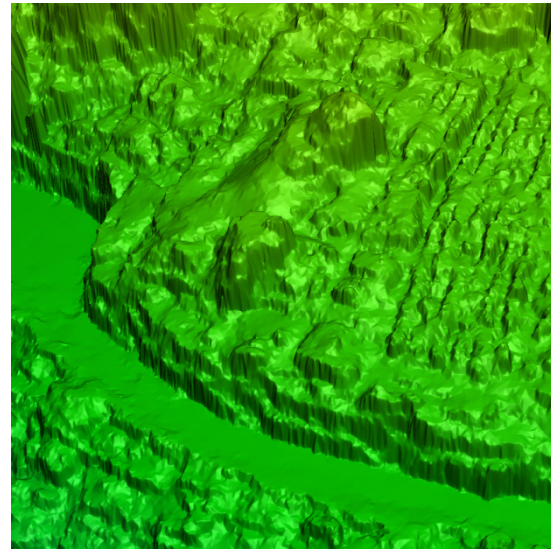
The small sample area shows a small part of the vineyard and the one lane country road which is used by the farmers to reach their fields (Figure 6). The steep walls on the one side of the road are seen, where stairs to reach the higher vineyards are directly integrated. The upper left part of this figure shows the DSM derived from SURE with texture. The details are clearly visible, even the single vine rows can be detected. Remember, the flight was done in August, with leaves on vegetation. The situation is different when looking on the Pix4D DSM (upper right). The fine structures are not fully modeled (see the vine rows and the stairs in the steep walls). This becomes more visible, if both DSMs are overlaid as shown in the lower left part of the figure. The Pix4D DSM is more smoothed, the single vine rows from SURE DSM are visible like peaks in the surface. Within the lower right part the color coded differences between SURE and Pix4D surfaces are given. The green colors belong to those parts, where the differences are between $>-30\text{cm}$ and $<30\text{cm}$. When the amount of the difference is below/above $\pm 1.6\text{m}$, no color coding is done. This is why the large differences remain grey. The red colors indicate those regions where the difference is between $0.3\text{m} - 1.6\text{m}$, i.e. the Pix4D DSM is higher than the SURE surface. Vice versa, the blue colored parts indicate those regions where the difference is between $-1.6\text{m} - -0.3\text{m}$, i.e. the Pix4D surface is above the SURE surface.

These comparisons give a first feeling how consistent both surfaces are, still, it does not give a measure on the accuracy of each individual surface. Typically the quality of 3D surface models is obtained from 3D reference surfaces. Man-made structures, like buildings or other 3D objects of sufficient size are well suited for such investigations. Unfortunately, as it was not allowed to fly over built-up areas, there are hardly any of those objects in the very rural mission site. There are a

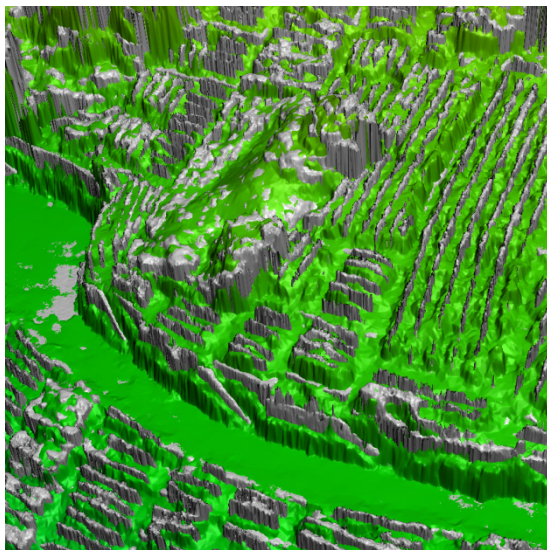
few very small buildings but many of those are partly covered by vegetation and not really visible from the air. In addition, their size is too small to allow for a comprehensive statistical analysis of 3D quality of DSM. On the other hand, the standard official DTM from the national mapping obtained from airborne LiDAR only offers 1m resolution and refers to the interpolated terrain not the surface. Its accuracy is specified to be better than 0.5 m. With that it also cannot serve as a reference.



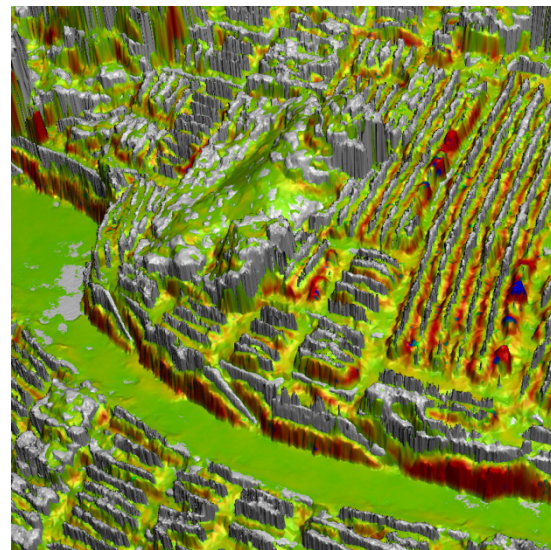
DSM SURE (textured)



DSM Pix4D



Overlay DSM SURE (grey) & Pix4D (green)



Differences DSM SURE – Pix4D

Figure 6: Comparison between SURE and Pix4D surface models.

Finally, only the relative accuracy (noise level) of defined areas within the reconstructed DSMs has been investigated. This noise analyses are derived from defined polygons on (assumed) planar surfaces, namely streets. There are two paved streets in the test site, the first one is the small 1-lane country road (in the higher part of the site, named upper road), the other one is a two lane country road close to the river (lower road). Both roads can be seen in Figure 5. 20 polygons are defined in the “upper road” and another 10 polygons in the “lower road” (Figure 7). After polygons have been defined, all the points from the different DSMs are extracted within each of the polygons. The extracted points are then used to estimate a 3D best fitting plane for each polygon. A possible

curvature of the road surface perpendicular to the direction of travel (road profile) is neglected here. It is about 3000 – 9000 points per polygon (depending on the slightly different polygon size) used for each plane estimation. Finally the height difference of each extracted DSM point to this estimated plane is analysed. The results can be seen in Table 2. The mean / median reflects the mean / median of std.devs. of vertical differences for each plane for the upper and lower road, respectively. Due to the varying image scale the polygons of lower and upper road were examined separately. Notice, in order to get robust results, outliers (i.e. points with height difference $>3\sigma$ to the plane within one polygon) have been eliminated before the differences are statistically analysed. The variation between the std.dev. of single planes is reflected in the std.dev. value (i.e. std.dev. of std.dev. from 20 and 10 planes respectively). This value shows the consistency of results.

The results in Table 2 confirm, what already was discussed in Figure 6. The SURE DSM seems to be of slightly higher (relative) accuracy. The mean / median are smaller than the values derived for the Pix4D DSM. The results for the upper road are slightly better than for the lower road, which is due to the change in image scale because of the height difference. This is overlaid by the fact, that the 2-lane lower road might have a more pronounced road profile compared to the upper road. The results from SURE also are more consistent, i.e. the variations between individual std.dev. in each plane is smaller. This also can be seen from the minimum and maximum values. In Figure 8 the color coded difference between the SURE and Pix4D DSM is given for two selected polygons of upper road. Please notice the different color scales. For polygon 7 (left) the estimated std.dev. (i.e. difference from estimated plane) is 15mm and 25mm for SURE and Pix4D, respectively. This is almost similar to the overall median in Table 2. The maximum difference between both DSMs is around 15cm. The Pix4D DSM is slightly above the SURE DSM. Polygon 3 (right) shows the problem of smoothing in the Pix4D DSM. Here large deviations up to almost 3m are seen in the difference, which is due to smoothing effects in Pix4D DSM. This also influences the std.dev. which reaches 132mm (max. value in Table 2) for the Pix4D points. The std.dev. of SURE points within this polygon again is around 20mm.



Figure 7: Planar test areas to determine the relative accuracy (std.dev., noise) of DSM (vertical component). Not all the defined polygons, only those in centre part of the test areas are shown.

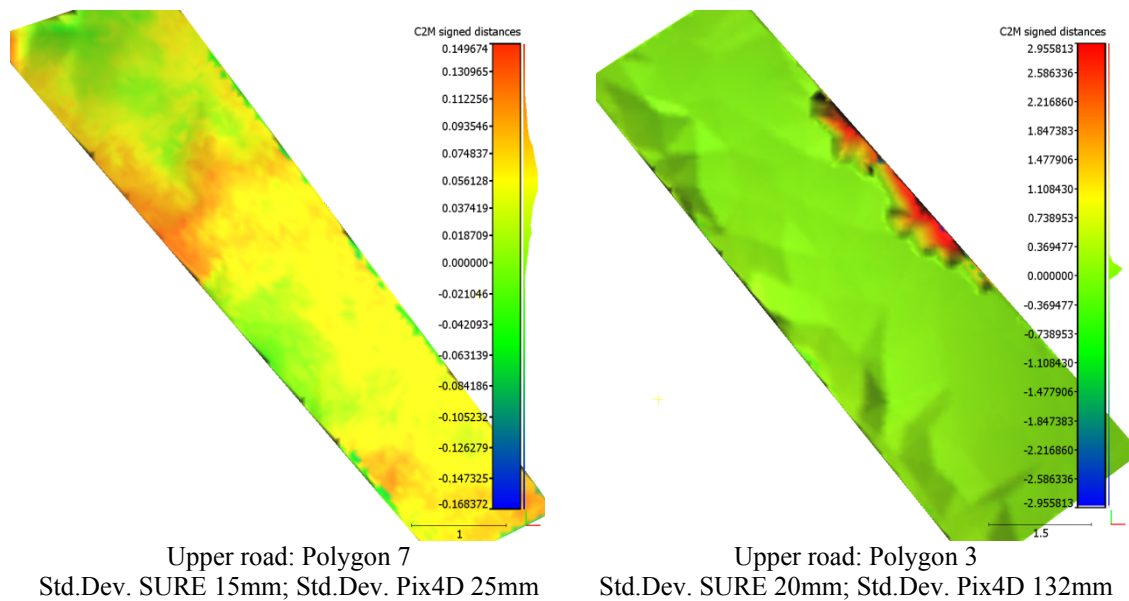


Figure 8: Noise analysis, color coded difference between SURE and Pix4D DSM.

	Upper Road 20 polygons, in [mm]		Lower road 10 polygons, in [mm]	
	SURE	Pix4D	SURE	Pix4D
mean	19.0	36.1	20.8	44.7
median	19.2	26.8	17.5	42.2
std.dev.	6.2	27.6	5.8	13.9
max	36.4	132.1	29.5	79.7
min	9.5	3.9	14.6	31.0

Table 2: Relative accuracy (std.dev., noise) of DSM (vertical component).

Generally SGM stereo mapping in low texture areas, as it the case for the selected 30 test regions (paved road surface), tends to rather do a smoothing of the reconstructed surface. Other areas with widely varying heights are expected to show a slightly higher measurement noise as derived here. However, the standard deviation (noise) in the range of $\frac{1}{2}$ GSD as obtained by SURE is quite impressive for this type of application. The Pix4D DSM generation in general showed slightly worse results, but as the software is constantly being improved and the dense surface model generation is one of their main issues, it is expected to also have a more powerful DSM generation within Pix4D in near future. Thus results here only reflect a “performance snap-shot” as it is the case for all the other involved software and hardware too.

5. SUMMARY

This paper showed the main results of the first German pilot study using UAS in the context of national mapping. Focus was laid on the use of UAS in the application field of land consolidation which is one of the possible applications for UAS in national mapping.

Within this project two different UAS fixed-wing platforms (micro category), including two different camera systems have been tested. Furthermore two independent process lines have been used for the data processing. The more standard photogrammetric processing using Match-AT (after pre-processing of images) is compared to a SFM approach from computer vision, implemented in

the Pix4D software. The surface models are derived by dense matching, the SURE software and the Pix4D surface model processing, which is inherent part of the software.

The absolute accuracy from check point analysis after image orientation is very sufficient and both process lines obtain almost similar accuracy. It has been shown that even with such relatively simple cameras and UAS platforms 3D object point determination in the sub-pixel range (absolute accuracy) is possible. The Match-AT processing needs some pre-processing to overcome the larger variations from nadir direction, which affects the assumption on initial starting values; it is assumed that future Match-AT versions will be able to also handle this type of image blocks without need for pre-processing. Still Match-AT offers the full photogrammetric capabilities and people from national mapping are more used to this type of processing software. The Pix4D on the other hand is especially designed to handle UAS imagery. It is straight forward, as most of the processing is done fully automatically with hardly any user interaction. Camera calibration is always included during processing to optimize and fully control interior geometry of the typically less stable consumer grade cameras used. Still, compared to the Match-AT approach, the manual measuring of image points is less user friendly, and a thorough error analysis of adjustment results is not yet part of the software.

The results from surface generation using SURE and Pix4D are slightly different. In both cases surface models with one pixel resolution (grid cell size about 6cm) were generated, still the Pix4D DSM generator (version 2.2.3) performed slightly worse compared to the SURE processing. SURE allows for (relative) accuracy in the range of $\frac{1}{2}$ pix. The absolute accuracy could not be checked, as no appropriate 3D features for DSM performance testing were available.

The UAS fixed-wing installation very reliably was flown in this project. The image data was captured as planned. Fixed-wing should be preferred for missions like this. Still, due to the terrain shape, some of the details especially on the steep parts could not be reconstructed because of occlusions. This could be solved by oblique imagery, which easily can be taken from rotary-wing platforms. Such platforms allow for an easy tilting of the camera platform and might be used in addition to fixed-wing UAS, in especially when such steep areas have to be reconstructed in detail. Furthermore, these rotary-wing platforms are favored for the reconstruction of single 3D objects. In this context the LGL BW especially asked for detailed modeling of some of the steep rocks, which are also used for rock climbing. This special task could not be solved with the fixed wing carriers.

Based on the results of the study, the UAS-based data acquisition for operational applications in the context of national mapping can be regarded as successful. The requested products have been derived; the accuracy could be met, sometimes even over-fulfilled. The flexible use of such platforms, however, was limited by the requested time to get permission to flight. This somehow limits the use especially for those applications flown in flying heights of more than 100m above ground and applications in built-up areas. Flight regulation issues are not discussed in this paper, but there are several national and European initiatives working on the integration of UAS in the civilian airspace. This for sure will simplify and harmonize all the procedures for obtaining approvals to use UAS in civilian operational context.

6. ACKNOWLEDGEMENTS

Special thanks needs to be expressed to the LGL Baden-Württemberg for funding this study. The LGL employee Mr. Gültlinger and Mr. Hummel always gave their best possible support to us in the practical implementation of the study at any time. This should be especially emphasized. Also the support of my colleagues at ifp and especially the colleagues from the iFR, namely Mr. Trittler and Mr. Weimer is acknowledged. Without their active participation, the UAS flights could not be performed. Mr. Ehrle was always available as expert model aircraft pilot to carry out the aerial surveys missions. The contribution of Mr. Leinss is particularly highlighted. Mr. Leinss was deeply

involved in this project as part of his thesis research work and was primarily responsible for the quality inspection of the camera systems and their integration into the aircraft platforms. He did an excellent job! The support of Pix4D is cordially mentioned. All the Pix4D results were obtained by Pix4uav Desktop 3D 2.2.3, which kindly was made available to ifp.

7. BIBLIOGRAPHY

- Abdel-Wahab, M., Wenzel, K. & Fritsch, D. (2011): Reconstruction of Orientation and Geometry from large Unordered Datasets for Low Cost Applications. – LC3D Workshop, Berlin.
- Abdel-Wahab, M., Wenzel, K. & Fritsch, D. (2012): Efficient Reconstruction of Large Unordered Image Datasets for High Accuracy Photogrammetric Applications. – ISPRS Annals of the Photogrammetry, Remote Sensing and Spatial Information Sciences I (3): pp. 1-6, Melbourne, Australia.
- Blyenburgh, P. (2012): RPAS Yearbook 2012/13 – The global perspective. http://www.uvs-info.com/index.php?option=com_flippingbook&view=book&id=13&page=1&Itemid=686 (19.7.2013).
- Blyenburgh, P. (2013): RPAS Yearbook 2013/14 – The global perspective. http://www.uvs-info.com/index.php?option=com_content&view=article&id=244&Itemid=280 (19.7.2013).
- Bormatec, (2013): http://bormatec.com/index.php?option=com_content&view=article&id=78&Itemid=59&lang=en (19.7.2013).
- Cramer, M., Haala, N., Rothermel, M., Leinss, B. & Fritsch, D. (2013a): UAV-gestützte Datenerfassung für Anwendungen der Landesvermessung – das Hessigheim-Projekt. – 33. DGPF-Jahrestagung, 3-Ländertagung: pp. 450-469, Freiburg.
- Cramer, M., Bovet, S., Gültlinger, M., Honkavaara, E., McGill, A., Rijdsdijk, M., Tabor, M. & Tournadre, V. (2013b): On the use of RPAS in national mapping – the EuroSDR point of view. Paper to be published in proceedings of UAV-g 2013 Conference, Rostock, September 4-6, 2013.
- Cramer, M., Haala, N., Rothermel, M., Leinss, B. & Fritsch, D. (2013c): UAV@LGL – Pilotstudie zum Einsatz von UAV im Rahmen der Landesvermessung in Deutschland. Report submitted to Photogrammetrie – Fernerkundung – Geoinformation (PFG), ISSN 1432-8364, Journal for Photogrammetry, Remote Sensing and Geoinformation Science.
- Farenzena, M., Fusiello, A. & Gherardi, R. (2009): Structure and motion pipeline on a hierarchical cluster tree. – ICCV Workshop on 3-D Digital Imaging and Modeling: pp. 1489-1496.
- Haala, N., (2011): Multiray Photogrammetry and Dense Image Matching. – Fritsch, D. (Ed.), Photogrammetric Week '11: pp. 185-195, Wichmann.
- Hirschmüller, H., (2008): Stereo Processing by Semi-Global Matching and Mutual Information. – IEEE Transactions on Pattern Analysis and Machine Intelligence 30 (2): pp. 328-341.

- Küng, O., Strecha, C., Beyeler, A., Zufferey, J.-C., Floreano, D., Fua, P. & Gervais, F. (2011): The accuracy of automatic photogrammetric techniques on ultra-light UAV imagery. – IAPRS XXXVIII-1/C22, UAV-g 2011: pp. 1-6, Zurich, Switzerland.
- Remondino, F. (2006): Detectors and descriptors for photogrammetric applications. – IAPRS XXXVI (3): pp. 1-6, Bonn.
- Rothermel, M., Wenzel, K., Fritsch, D. & Haala, N. (2012): SURE: Photogrammetric Surface Reconstruction from Imagery. – LC3D Workshop 2012, Berlin.
- Snavely, N., Seitz, S. & Szeliski, R. (2008): Modeling the World from Internet Photo Collections. – International Journal of Computer Vision 80 (2): pp. 189-210.
- Strecha, C., Fletcher, A., Lechner, A., Erskine, P. & Fua, P. (2012): Developing species specific vegetation maps using multi-spectral hyperspatial imagery from unmanned aerial vehicles, ISPRS Ann. Photogramm. Remote Sens. Spatial Inf. Sci., I-3, 311-316, 2012. <http://www.isprs-ann-photogramm-remote-sens-spatial-inf-sci.net/I-3/311/2012/isprsannals-I-3-311-2012.pdf> (19.7.2013).
- UAV-g (2011): Proceedings of the International Conference on Unmanned Aerial Vehicle in Geomatics (UAV-g), Editor(s): H. Eisenbeiss, M. Kunz, and H. Ingensand, September 14–16, Zurich, Switzerland, ISPRS Archives – Volume XXXVIII-1/C22, 2011. <http://www.int-arch-photogramm-remote-sens-spatial-inf-sci.net/XXXVIII-1-C22/> (19.7.2013).
- van Persie, M., Rijdsdijk, M., van Hinsbergh, W. H. M., Witteveen, W., ten Buuren, G. H. M., Schakelaar, G. A., Poppinga, G. & Ladigues, R. (2013): Unmanned aerial systems in the process of juridical verification of cadastral borders. Paper to be published in proceedings of UAV-g 2013 Conference, Rostock, September 4-6, 2013.